

## Relative importance of organic coatings for the heterogeneous hydrolysis of $N_2O_5$ during summer in Europe

N. Riemer,<sup>1</sup> H. Vogel,<sup>2</sup> B. Vogel,<sup>2</sup> T. Anttila,<sup>3</sup> A. Kiendler-Scharr,<sup>4</sup> and T. F. Mentel<sup>4</sup>

Received 27 October 2008; revised 25 March 2009; accepted 23 June 2009; published 15 September 2009.

[1] The heterogeneous reaction probability  $\gamma_{N_2O_5}$  of  $N_2O_5$  depends largely on the aerosol chemical composition. Several recent laboratory studies have shown that the presence of organic coatings on aqueous aerosols can suppress heterogeneous  $N_2O_5$  hydrolysis. In this study we investigated the relative importance of organic coatings, formed via gas-to-particle conversion on aqueous aerosols, to  $N_2O_5$  hydrolysis on local and regional scales during summer in Europe. We present results of one-dimensional process studies and of regional-scale model simulations for Europe with the comprehensive model system COSMO-ART. To treat  $N_2O_5$  hydrolysis, we used recent results from laboratory studies that quantified  $\gamma_{N_2O_5}$  on the basis of the organic coating thickness. The simulations showed that during any episode the conditions for formation of  $N_2O_5$  and secondary organic compounds were very variable and depended strongly on the meteorological conditions. In regions of the model domain where both components were built-up, the formation of organic coatings could decrease particulate nitrate concentrations by up to 90%. Where these conditions were not met, the impact of the organic coating was negligible.

**Citation:** Riemer, N., H. Vogel, B. Vogel, T. Anttila, A. Kiendler-Scharr, and T. F. Mentel (2009), Relative importance of organic coatings for the heterogeneous hydrolysis of  $N_2O_5$  during summer in Europe, *J. Geophys. Res.*, 114, D17307, doi:10.1029/2008JD011369.

### 1. Introduction

[2] Aerosol particles influence atmospheric chemistry by providing a medium for chemical reactions that take place on the aerosol surfaces or in the aerosol liquid phases [Ravishankara and Longfellow, 1999; Jacob, 2000]. An important reaction in this respect is the heterogeneous hydrolysis of  $N_2O_5$ , which forms a major sink of nitrogen oxides in the night [Jacob, 2000; Brown *et al.*, 2004]. For the global scale it has been demonstrated that  $N_2O_5$  hydrolysis affects the budgets of nitrogen oxides and ozone and thereby impacts the oxidizing capacity of the atmosphere [Dentener and Crutzen, 1993; Evans and Jacob, 2005]. For the regional to the continental scale and for summer conditions, Riemer *et al.* [2003b] showed that the impact of heterogeneous  $N_2O_5$  hydrolysis causes remarkable changes in the nocturnal concentrations of nitrogen-containing species and on aerosol properties such as the surface area concentration and nitrate content. Numerous laboratory studies have also shown that the rate of  $N_2O_5$  reactive uptake depends crucially on the size, phase and chemical composition of aerosols [Mozurkewich and Calvert, 1988;

Wahner *et al.*, 1998b; Folkers *et al.*, 2003; Thornton *et al.*, 2003; Badger *et al.*, 2006; McNeill *et al.*, 2006; Davis *et al.*, 2008, and references therein], all of which exhibit large variability in the atmosphere. This variability and its impact on the particle reactivity should also be accounted for in large-scale models simulating atmospheric chemistry [Evans and Jacob, 2005; Brown *et al.*, 2006].

[3] Recent experimental research has shown that organic coatings on aerosol particles can affect heterogeneous reactions. [Folkers *et al.*, 2003; Badger *et al.*, 2006; Thornton and Abbatt, 2005; McNeill *et al.*, 2006; Anttila *et al.*, 2006, 2007; Cosman *et al.*, 2008]. Particles can be emitted with an organic coating, as has been suggested for sea salt aerosols [Ellison *et al.*, 1999]. Alternatively, the organic coatings may be formed in the atmosphere by secondary organic aerosol from biogenic emissions [Folkers *et al.*, 2003; Anttila *et al.*, 2007]. Depending on the formation mechanism, such layers may consist of a single layer of molecules (monolayered coatings) or of several molecule layers (multilayered coatings). Gill *et al.* [1983] suggested already in 1983 that atmospheric particles can have organic coatings that are of importance. Evidence for particles coated with organics in the atmosphere was presented by Mochida *et al.* [2002], Russell *et al.* [2002], and Tervahattu *et al.* [2002a, 2002b, 2005]. These experimental findings motivate detailed modeling studies to quantify the influence of coated particles on atmospheric chemistry. However, with the exception of the work of Smoydzin and von Glasow [2007], no such studies have been conducted to date. In particular, there is a lack of studies focusing on the impact of organic coatings on  $N_2O_5$  hydrolysis on the regional or global scale.

<sup>1</sup>Department of Atmospheric Sciences, University of Illinois at Urbana-Champaign, Urbana, Illinois, USA.

<sup>2</sup>Institut für Meteorologie und Klimaforschung, Forschungszentrum Karlsruhe, Eggenstein-Leopoldshafen, Germany.

<sup>3</sup>Climate and Global Change, Research and Development, Finnish Meteorological Institute, Helsinki, Finland.

<sup>4</sup>ICG-II: Troposphere, Forschungszentrum Jülich, Jülich, Germany.

[4] In current atmospheric models, the rate of a heterogeneous reaction is quantified on the basis of the aerosol surface area and the so-called uptake coefficient or reaction probability  $\gamma$ . The quantity  $\gamma$  can be viewed as the probability that a molecule colliding with the particle surface will react either on the particle surface or within the particle volume. The values of uptake coefficients for various systems can be determined from measurements. Furthermore, there are theoretical frameworks that can be used to calculate the uptake coefficient as a function of the rates of the individual processes involved in the uptake [e.g., *Hanson et al.*, 1994; *Pöschl et al.*, 2007]. These frameworks facilitate the interpretation of experimental data and allow for extrapolating results from laboratory studies to a wider range of conditions. Recently, *Anttila et al.* [2006] developed an uptake formalism that can be applied to calculate the N<sub>2</sub>O<sub>5</sub> uptake coefficient for a particle containing an aqueous core surrounded by a multilayered organic coating, on the basis of the physicochemical properties of the coated particle and the reactive molecule. This model was applied to explain the suppression of N<sub>2</sub>O<sub>5</sub> hydrolysis in aqueous aerosols coated with monoterpene oxidation products that has been observed in laboratory experiments. The results showed that such coatings reduce the reactivity of N<sub>2</sub>O<sub>5</sub> significantly. Also the Henry's law constant and the diffusion constant of N<sub>2</sub>O<sub>5</sub> for the organic coating are decreased, compared to noncoated aqueous aerosols. These findings serve as motivation to investigate the effects that the formation of such coatings may have on atmospheric chemistry.

[5] In this study, we incorporated the framework of *Anttila et al.* [2006] into a comprehensive regional chemistry transport model [*Riemer et al.*, 2003a; *Vogel et al.*, 2008]. The main aim was to quantify the effect of organic coatings on N<sub>2</sub>O<sub>5</sub> heterogeneous hydrolysis on local and regional scales. We focused on a situation in summer to allow higher biogenic emissions and therefore higher secondary organic aerosol formation. In our study we assumed that the organic coatings were formed by gas-to-particle conversion; that is, they were of secondary nature. We also assessed the sensitivity of the results to the ambient NO<sub>x</sub> concentration levels and to the assumption of the organic matter forming a film versus partially dissolving in the bulk of the particle. The manuscript is organized as follows. Section 2 reviews the background on the relevant reactions involved in heterogeneous N<sub>2</sub>O<sub>5</sub> hydrolysis and presents our parameterization of  $\gamma_{\text{N}_2\text{O}_5}$  for aerosols consisting of an inorganic core and an organic coating. In section 3 we describe the application of this parameterization in a one-dimensional model system and present the results of the process studies. In section 4 we present the implementation of the parameterization in the comprehensive three-dimensional model system COSMO-ART and evaluate the relative importance of the organic coating for a photosmog episode on a regional scale. Section 5 concludes our findings.

## 2. Model Representation of the Heterogeneous Hydrolysis of N<sub>2</sub>O<sub>5</sub>

[6] During the day the most important removal path for NO<sub>x</sub> in the atmosphere is the formation of HNO<sub>3</sub> by the reaction of NO<sub>2</sub> and OH:



Reaction (R1) also provides an important loss mechanism for OH under polluted conditions. The appearance of NO<sub>3</sub> is characteristic of nighttime chemistry. It is formed by the reaction of NO<sub>2</sub> and O<sub>3</sub>:



NO<sub>3</sub> further reacts with NO<sub>2</sub> to form N<sub>2</sub>O<sub>5</sub>. Owing to rapid photolysis, significant concentrations of NO<sub>3</sub>, and hence N<sub>2</sub>O<sub>5</sub>, can only be reached during the night. N<sub>2</sub>O<sub>5</sub> is thermally unstable and decomposes back to NO<sub>2</sub> and NO<sub>3</sub>, so we have the following two reactions:



NO<sub>3</sub> reacts with a number of volatile organic compounds (VOC) such as monoterpenes and phenols and initiates the formation of peroxy and hydroxy radicals [*Platt et al.*, 1990; *Mihelcic et al.*, 1993] and finally organic nitrates and nitric acid [*Wayne et al.*, 1991]:



[7] While the reaction of N<sub>2</sub>O<sub>5</sub> with water vapor is very slow [*Tuazon et al.*, 1983; *Wahner et al.*, 1998a], N<sub>2</sub>O<sub>5</sub> reacts relatively rapidly on and in aqueous aerosol particles [*Platt et al.*, 1984; *Mozurkewich and Calvert*, 1988]:



The heterogeneous hydrolysis of N<sub>2</sub>O<sub>5</sub> thus provides a removal path for NO<sub>x</sub> and competes with reaction (R4). Reaction (R6) is usually implemented into chemical transport models as a first-order loss by

$$\left. \frac{d[\text{N}_2\text{O}_5]}{dt} \right|_{\text{het}} = -k_{\text{N}_2\text{O}_5} [\text{N}_2\text{O}_5]. \quad (1)$$

The surface-area-dependent rate constant  $k_{\text{N}_2\text{O}_5}$ , which is necessary for a quantitative treatment of reaction (R6), is usually parameterized by

$$k_{\text{N}_2\text{O}_5} = \frac{1}{4} c_{\text{N}_2\text{O}_5} S \gamma_{\text{N}_2\text{O}_5}, \quad (2)$$

where  $c_{\text{N}_2\text{O}_5}$  is the mean molecular velocity of N<sub>2</sub>O<sub>5</sub> and  $S$  is the aerosol surface area concentration. Our method for calculating  $\gamma_{\text{N}_2\text{O}_5}$  as a function of the aerosol chemical composition is described in section 2.2.

### 2.1. Aerosol Module MADEsoot

[8] For the one-dimensional and three-dimensional models presented in this study, we used the aerosol module MADEsoot [*Riemer et al.*, 2003a]. MADEsoot is based on the Regional Particulate Model (RPM) [*Binkowski and Shankar*, 1995] and provides detailed information about the chemical composition and size of atmospheric particles

as well as the dynamic processes influencing the size distributions.

[9] The aerosol population of the submicron particles was represented by several overlapping modes, which are approximated by lognormal functions. In the model version used here we considered secondary inorganic and organic aerosol, as well as soot in two different mixing states (externally and internally mixed). Specifically, we represented the aerosol distribution by five modes: one mode for externally mixed soot, two soot-free modes containing SO<sub>4</sub><sup>2-</sup>, NH<sub>4</sub><sup>+</sup>, NO<sub>3</sub><sup>-</sup>, water and secondary organic aerosol (SOA) in an internal mixture, and two modes containing soot and SO<sub>4</sub><sup>2-</sup>, NH<sub>4</sub><sup>+</sup>, NO<sub>3</sub><sup>-</sup>, water and SOA in an internal mixture. The treatment of soot in this framework, which encompasses the transfer of soot from the externally mixed soot mode to the soot-containing modes, is described in detail by *Riemer et al.* [2003a]. If the relative humidity was high enough so that water was present in the aerosol, we assumed that the inorganic species formed an aqueous solution and only then would hydrolysis of N<sub>2</sub>O<sub>5</sub> occur. The formation of SOA was calculated with the SORGAM scheme [*Schell et al.*, 2001]. SORGAM treats anthropogenic and biogenic gas phase precursors separately. As anthropogenic precursors we considered toluene, xylene, cresol, higher alkanes and higher alkenes. The biogenic precursors were  $\alpha$ -pinene and limonene. The gas-particle partitioning of SOA compounds was parameterized with a two-component model [*Odum et al.*, 1996]. Furthermore, the binary nucleation of sulfuric acid and water, coagulation, condensation, turbulent diffusion, deposition, and the emission of soot aerosol were among the simulated dynamical processes that modified the aerosol population spatially and temporally. The aerosol surface area concentration and the aerosol composition, and therefore  $k_{N_2O_5}$ , were time- and height-dependent. In this study, we did not consider mineral dust and sea salt aerosol.

## 2.2. Calculation of the Reaction Probability $\gamma_{N_2O_5}$ Including an Organic Coating

[10] In this paper we focus on the impact of organic coatings on the heterogeneous hydrolysis of N<sub>2</sub>O<sub>5</sub>. For the calculation of the overall  $\gamma_{N_2O_5}$  used in equation (2) we adopted the following method. The overall  $\gamma_{N_2O_5}$  is the surface-weighted average over all  $N$  aerosol modes:

$$\gamma_{N_2O_5} = \sum_{i=1}^N \frac{S_i}{S} \gamma_i, \quad (3)$$

where  $S_i$  is the surface area concentration of mode  $i$  and  $S$  is the total surface area, formed by summing  $S_i$  over all  $N$  modes. To calculate  $S$ , we included the primary particulate matter, the secondary particulate matter, and particle-bound water.

[11] If a mode contained SOA then we assumed that this organic material formed a coating that surrounded the inorganic core. This meant that all the condensed organic material contributed to the coating, and in this sense the calculations represent an extreme scenario. There exists evidence for the formation of coatings of SOA on aqueous aerosol under laboratory conditions [e.g., *Anttila et al.*, 2007]. Furthermore, hygroscopic growth measurements show that at relative humidity below 60% the water uptake

of SOA resulting from oxidation of biogenic volatile organic compounds is negligible [*Varutbangkul et al.*, 2006; *Saathoff et al.*, 2003], which supports the assumption on the formation of coatings made here. On the other hand, our current knowledge of the extent of water solubility of atmospheric SOA is limited and the possibility cannot be excluded that atmospheric SOA partly or entirely dissolves into the aerosol aqueous phase. More research on this topic is needed to refine this assumption in the future, but we explore the sensitivity of the results with respect to assumptions regarding the water solubility of SOA below.

[12] Given a mode  $i$ , we expressed the reaction probability of this mode,  $\gamma_i$ , by the expression derived by *Anttila et al.* [2006]:

$$\frac{1}{\gamma_i} = \frac{1}{\gamma_{i,\text{core}}} + \frac{1}{\gamma_{i,\text{coat}}}. \quad (4)$$

For  $\gamma_{i,\text{core}}$ , which describes the reaction probability of the inorganic core of the aerosol particles, we used the parameterization from our previous study [*Riemer et al.*, 2003b]:

$$\gamma_{i,\text{core}} = f\gamma_1 + (1-f)\gamma_2, \quad (5)$$

with  $\gamma_1 = 0.02$ ,  $\gamma_2 = 0.002$ , and  $f = \frac{m_{SO_4}}{m_{SO_4} + m_{NO_3}}$ .

[13] Here  $m_{SO_4}$  and  $m_{NO_3}$  are the aerosol mass concentrations of sulfate and nitrate. This parameterization for  $\gamma_{i,\text{core}}$  accounts for the fact that the reaction probability is of the order of one magnitude lower if the aerosol contains nitrate rather than sulfate [*Mentel et al.*, 1999]. To include this effect we used the weighting in equation (5) of the reaction probabilities according to the nitrate versus sulfate content of the aerosol, as introduced by *Riemer et al.* [2003b].

[14] *Davis et al.* [2008] proposed an extended parameterization for hydrolysis on inorganic aerosols that includes the dependence on relative humidity and temperature. However, in this study we did not take into account these dependencies to ease the interpretation of the results in terms of the effect of the organic coatings.

[15] For  $\gamma_{i,\text{coat}}$  we used the formulation according to *Anttila et al.* [2006]:

$$\gamma_{i,\text{coat}} = \frac{4RTH_{\text{org}}D_{\text{org}}R_{c,i}}{c_{N_2O_5}\ell_iR_{p,i}}, \quad (6)$$

where  $R$  is the universal gas constant,  $T$  is the temperature,  $H_{\text{org}}$  is the Henry's Law constant of N<sub>2</sub>O<sub>5</sub> for the organic coating, and  $D_{\text{org}}$  is the diffusion coefficient of N<sub>2</sub>O<sub>5</sub> in the organic coating. As in the paper by *Anttila et al.* [2006],  $R_{p,i}$ ,  $R_{c,i}$ , and  $\ell_i$  are the radius of the particle, the radius of the core, and the thickness of the coating, respectively. In their experiment, the particle size was measured, the core size and layer thickness were derived from experimental data, and the organic coatings were produced through condensation of low-volatility vapors formed through monoterpene ozonolysis. In our model simulations we used the corresponding calculated values as further described below. The quantities  $H_{\text{org}}$  and  $D_{\text{org}}$  depend on the physicochemical properties of compounds comprising the coating. The product  $H_{\text{org}}D_{\text{org}}$  can be derived from experimental data as

described by *Anttila et al.* [2006]. For these two parameters, we used values that are consistent with the analysis presented by *Anttila et al.* [2006], who showed that the product  $H_{\text{org}}D_{\text{org}}$  is about  $0.03H_{\text{aq}}D_{\text{aq}}$  for organic coatings consisting of condensed monoterpene oxidation products. Here  $H_{\text{aq}}$  is the Henry's law constant of N<sub>2</sub>O<sub>5</sub> for the aqueous phase ( $H_{\text{aq}} = 5000 \text{ M atm}^{-1}$ ) and  $D_{\text{aq}}$  is the diffusion coefficient of N<sub>2</sub>O<sub>5</sub> in the aqueous phase ( $D_{\text{aq}} = 10^{-9} \text{ m}^2 \text{ s}^{-1}$ ). Equations (4) and (6) represent a simpler formulation of the full solution for the reactive uptake by a coated particle. They parameterize the rate of reactive uptake for coatings that are relatively thin compared to the size of the particle aqueous core, and for coatings that are not reactive with N<sub>2</sub>O<sub>5</sub> [*Anttila et al.*, 2006]. In particular, coatings composed of water-insoluble compounds fulfill the latter criterion. The uncertainties in the experimental values of  $\gamma_{i,\text{coat}}$  were between 10% and 20% [*Anttila et al.*, 2006]. Regarding other uncertainties, there is not enough relevant experimental data on atmospheric, film-forming SOA at present to quantify the overall variability in  $\gamma_{i,\text{coat}}$  in the atmosphere. Therefore it is not meaningful to perform a more detailed study on the sensitivity of the results to the uncertainties in  $\gamma_{i,\text{coat}}$  at this time.

[16] Since we used a modal approach and assumed a complete internal mixture within the modes, we used the median radius with respect to the surface area distribution for  $R_{p,i}$  as representative of the distribution. We deduced  $R_{c,i}$  and  $\ell_i = R_{p,i} - R_{c,i}$  from the volume ratio  $\beta = V_{\text{inorg}} / (V_{\text{inorg}} + V_{\text{org}})$  of the inorganic material volume,  $V_{\text{inorg}}$ , and organic material volume,  $V_{\text{org}}$ , in the mode  $i$ :

$$\ell_i = R_{p,i} \left( 1 - \beta^{\frac{1}{3}} \right). \quad (7)$$

### 3. One-Dimensional Model Studies

[17] To systematically investigate the impact of an organic coating on N<sub>2</sub>O<sub>5</sub> hydrolysis, we first carried out one-dimensional process studies with the aerosol model MADEsoot coupled to the model system KAMM/DRAIS [*Adrian and Fiedler*, 1991; *Vogel et al.*, 1995], similar to our previous study described by *Riemer et al.* [2003b]. The advantage of using a 1-D model version compared to a more realistic 3-D model is that the complexity is reduced and the dominant factors are easier to identify and to interpret.

[18] KAMM/DRAIS uses the nonhydrostatic mesoscale model KAMM as a meteorological driver. The module DRAIS calculates the advection and diffusion of the reactive gas phase and the aerosol phase species. For the one-dimensional model version, only turbulent diffusion in the vertical direction was relevant. Dry deposition was included for both gas phase and aerosol phase species, following the big-leaf multiple-resistance model of *Bär and Nester* [1992]. The chemical reactions of the gaseous species were calculated using the chemical mechanism RADMKa, based on RADM2 [*Stockwell et al.*, 1990], but with updated reaction rates for  $\text{NO}_2 + \text{OH} \rightarrow \text{HNO}_3$  [*Donahue et al.*, 1997] and  $\text{HO}_2 + \text{NO} \rightarrow \text{OH} + \text{NO}_2$  [*Bohn and Zetzsch*, 1997]. Furthermore, the rate constants for  $\text{NO} + \text{OH} \rightarrow \text{HONO}$  were updated and a heterogeneous reaction that leads to the formation of HONO at surfaces was included [*Vogel et al.*, 2003]. The very simple isoprene scheme of

RADM2 was replaced by the more sophisticated one of *Geiger et al.* [2003]. Biogenic and anthropogenic hydrocarbons that may serve as precursors for secondary organic components of the aerosol were added to RADM2 using the SORGAM module by *Schell et al.* [2001]. The gas-phase hydrolysis of N<sub>2</sub>O<sub>5</sub> was not included. The vertical grid size varied from 17 m close to the surface to 400 m at the top of the model domain at 12 km above sea level, with a total of 45 vertical layers. The time steps were of the order of seconds. The whole model system ran in a fully coupled mode.

[19] We considered a cloudless situation under typical summer conditions with relative humidity above 55%. The anthropogenic gas phase emissions (NO<sub>x</sub>, NH<sub>3</sub>, CO, SO<sub>2</sub>, and the 32 categories of VOC in RADM2) were prescribed as time-dependent functions. They represented the conditions of a moderately polluted area in Europe [*Pregger et al.*, 2007]. We also included primary emissions of diesel soot, as described by *Riemer et al.* [2003a]. The biogenic VOC emissions were calculated on the basis of the land use, the modeled temperature, and the modeled radiative fluxes [*Vogel et al.*, 1995]. We investigated two emission scenarios: a low-NO<sub>x</sub> case and a high-NO<sub>x</sub> case. In the high-NO<sub>x</sub> case, the NO<sub>x</sub> emissions used for the low-NO<sub>x</sub> case were multiplied by a factor of 10, corresponding to a heavily polluted environment. These emission scenarios were considered because nitrate formation in aerosols has been shown to suppress the heterogeneous hydrolysis of N<sub>2</sub>O<sub>5</sub> [*Riemer et al.*, 2003b]. As shown later, this also affected the extent to which the N<sub>2</sub>O<sub>5</sub> hydrolysis rate is inhibited owing to the formation of organic coatings.

[20] We performed simulations for three cases: neglecting the heterogeneous hydrolysis of N<sub>2</sub>O<sub>5</sub> (case A), including the hydrolysis reaction but ignoring the impact of the organic coating (i.e.,  $\gamma_{\text{N}_2\text{O}_5} = \gamma_{\text{core}}$ ) (case B), and accounting for both the hydrolysis reaction and the formation of organic coatings as described by equations (3)–(6) (case C). As shown later, cases A and B represent the limiting cases in terms of NO<sub>x</sub> loss through reaction (R6), while case C falls between these extremes. The individual runs were carried out for several days to eliminate the influence of the initial conditions. We concentrate on the results of day 3 when the peak ozone concentrations reached values typical for summertime Central Europe.

[21] We first investigate the nighttime vertical profiles of those gas phase species and aerosol characteristics that were relevant for N<sub>2</sub>O<sub>5</sub> production or that were directly affected by the heterogeneous hydrolysis of N<sub>2</sub>O<sub>5</sub>. Figure 1 presents vertical mixing ratio profiles of NO<sub>2</sub>, the biogenic VOC  $\alpha$ -pinene (model species API), O<sub>3</sub>, NO<sub>3</sub>, N<sub>2</sub>O<sub>5</sub>, HNO<sub>3</sub>, the wet aerosol surface area concentration, SOA mass concentration, and the aerosol nitrate concentration at 0300 central European time (CET) for the low-NO<sub>x</sub> case and for the two different treatments of the heterogeneous hydrolysis of N<sub>2</sub>O<sub>5</sub>. At this time the stable nocturnal boundary layer had a height of 140 m, and the residual layer above reached 2000 m. NO<sub>2</sub>, O<sub>3</sub>, and NO<sub>3</sub> are presented because they are precursors of N<sub>2</sub>O<sub>5</sub>. HNO<sub>3</sub> is shown because it is a product of the heterogeneous hydrolysis of N<sub>2</sub>O<sub>5</sub>. Its gas phase concentration had an influence on the nitrate content of the aerosol. The species  $\alpha$ -pinene is shown as a representative of VOC because it is emitted during the night, it reacts

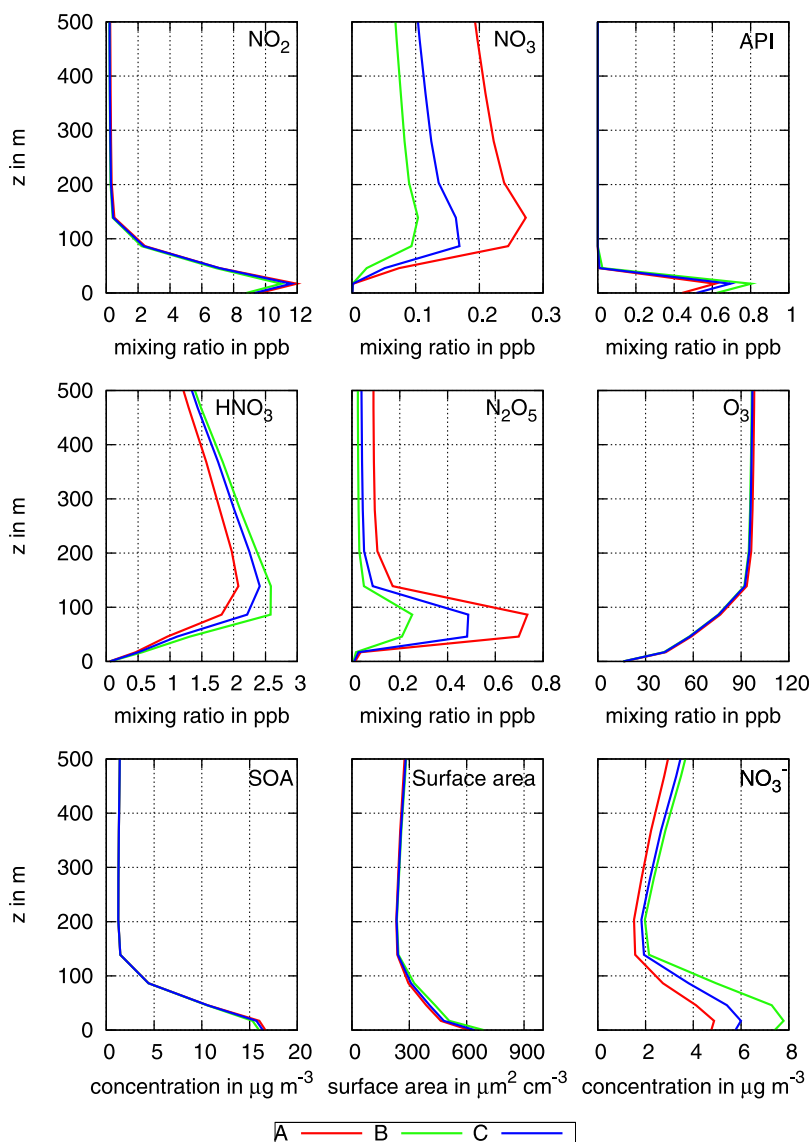


**Figure 1.** Simulated vertical profiles (at 0300 central European time, CET) of NO<sub>2</sub>, NO<sub>3</sub>,  $\alpha$ -pinene (API), HNO<sub>3</sub>, N<sub>2</sub>O<sub>5</sub>, O<sub>3</sub>, SOA, aerosol surface area, and aerosol nitrate for different parameterizations of heterogeneous hydrolysis: case A, neglecting hydrolysis; case B, including hydrolysis but ignoring organic coating; and case C, including hydrolysis and organic coating.

with NO<sub>3</sub>, and it is a precursor of SOA. The SOA profiles show the altitude at which the N<sub>2</sub>O<sub>5</sub> hydrolysis rate decreased considerably owing to the formation of organic coatings on particles. The aerosol surface area concentration determined the rate of hydrolysis of N<sub>2</sub>O<sub>5</sub> and is therefore also shown in Figure 1. Apart from ammonium nitrate and SOA, there was also ammonium sulfate present in the aerosol (not shown) with sulfate concentrations reaching values of about  $6 \mu\text{g m}^{-3}$  near the surface.

[22] The aerosol surface area concentration reached its maximum values in the upper part of the residual layer (around 1800 m; not visible in Figure 1) and close to the surface during the night. There are two reasons for this. First, the formation of ammonium nitrate contributed to the surface area depending on the availability of NH<sub>3</sub> and HNO<sub>3</sub>, on the temperature, and on the relative humidity (low temperature and high relative humidity favor the

formation of ammonium nitrate). Second, the uptake of water vapor that increased the aerosol surface area concentration was enhanced by high relative humidity. Both processes occurred in these layers. Near the ground SOA formation also contributed to the aerosol surface area. The SOA concentrations showed a pronounced maximum near the surface of about  $16 \mu\text{g m}^{-3}$ . The maximum was located near the surface since the SOA precursors were emitted close to the ground and since the low-volatility oxidation products were confined to the lowest layers owing to the ineffective vertical exchange. Within the nocturnal boundary layer the SOA concentrations declined, and increased slightly throughout the residual layer. The latter trend was due to the decreasing temperature, which favored the partitioning of the low-volatility oxidation products into the particle phase.

[23] Regardless of the hydrolysis treatment, the vertical profiles qualitatively exhibit the following features: NO<sub>2</sub>

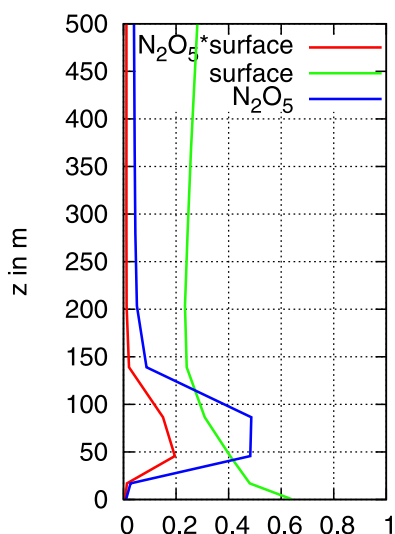


**Figure 2.** Vertical profiles of surface area  $S$  in  $\mu\text{m}^2 \text{cm}^{-3}$  (scaled by a factor of 0.001),  $\text{N}_2\text{O}_5$  mixing ratio in ppb, and the product  $\text{N}_2\text{O}_5 \cdot S$  in ppb  $\mu\text{m}^2 \text{cm}^{-3}$  (scaled by a factor of 0.001) at 0300 CET. All profiles are for case C (including hydrolysis and organic coating).

and  $\alpha$ -pinene had their maximum mixing ratios close to the surface since  $\text{NO}_x$  and  $\alpha$ -pinene were mainly emitted close to the surface. The mixing ratios of both  $\text{NO}_2$  and  $\alpha$ -pinene decreased with height, but the decrease in the mixing ratio of  $\alpha$ -pinene was steeper than that of  $\text{NO}_2$  because of the reaction of  $\alpha$ -pinene with  $\text{O}_3$  and  $\text{NO}_3$  and the ongoing conversion of  $\text{NO}$  to  $\text{NO}_2$  in those heights.

[24] During the night, ozone was depleted by the reaction with  $\text{NO}$  within the nocturnal boundary layer. The reduced vertical mixing, the reaction of ozone with freshly emitted  $\text{NO}$ , and the deposition of ozone at the surface all lead to a steep vertical gradient. Within the residual layer the high-ozone mixing ratios of the day before still existed.

[25]  $\text{NO}_3$  had a maximum at the top of the nocturnal boundary layer in the investigated case.  $\text{N}_2\text{O}_5$  was formed during the night, reaching its maximum mixing ratio at a height of approximately 50 m above the surface. Above 90 m,  $\text{N}_2\text{O}_5$  decreased very rapidly and was almost constant above 200 m in the residual layer. In contrast to  $\text{N}_2\text{O}_5$ ,  $\text{NO}_3$  decreased slowly with height.  $\text{HNO}_3$  had a maximum at 90 m above the surface. The shape of these profiles can be understood by analyzing the production and loss rates given by the reactions (R1)–(R6), which occurred with only little vertical transport in the stable nocturnal boundary layer. Such analysis was performed in detail in our previous study [Riemer et al., 2003b], and the results apply qualitatively to the present study. To summarize the main points, we note that the profile of  $\text{N}_2\text{O}_5$  was determined by the net effect of the rates of reactions (R3) and (R4) and by the heterogeneous hydrolysis of  $\text{N}_2\text{O}_5$  by reaction (R6). A maximum of production was determined by the coincident availability of  $\text{NO}_2$  and  $\text{NO}_3$ . The  $\text{NO}_3$  mixing ratio, in turn, was low near the surface because of the reaction of  $\text{NO}_3$  with internal alkenes, which had the highest mixing ratios near the surface. Moreover, the nighttime  $\text{O}_3$  surface mixing ratio was very low owing to the reaction with  $\text{NO}$ , with the result that  $\text{NO}_3$  could not be produced in that layer.

[26] A number of results from field observations have been published recently, confirming the observation of pronounced gradients in the  $\text{N}_2\text{O}_5$  and  $\text{NO}_3$  mixing ratios [Brown et al., 2007a, 2007b; Geyer and Stutz, 2004; Stutz et al., 2004]. Since  $\text{N}_2\text{O}_5$  hydrolysis has a reaction rate that depends on the product of surface area and  $\text{N}_2\text{O}_5$  mixing ratio (equations (1) and (2)), its relevance is limited to a region where both sufficient aerosol surface area and  $\text{N}_2\text{O}_5$  are present. The vertical profile of the product of surface area and  $\text{N}_2\text{O}_5$  mixing ratio, shown in Figure 2 for case C, illustrates this for the investigated conditions. Despite the large aerosol surface area near the ground, the rate of  $\text{N}_2\text{O}_5$  hydrolysis was negligible in this layer since the  $\text{N}_2\text{O}_5$  mixing ratios were very low. The maximum turnover occurred at a height of 40 m.

[27] We first briefly summarize the differences between the two limiting cases, A and B, and we then describe how the organic coating changes the picture. By comparing the vertical profiles corresponding to the cases A and B, the following conclusions can be drawn for the considered gas phase species (Figure 1). For case B,  $\text{N}_2\text{O}_5$  decreased by at most 70%, and by 50% near the ground, relative to case A. A similar comparison shows that the  $\text{NO}_3$  mixing ratio decreased by up to 70%, and by 45% near the ground. The impact of this reduction can be seen in the  $\alpha$ -pinene mixing ratio, which increased in case B compared to case A, since the loss due to the reaction with  $\text{NO}_3$  decreased. The aerosol nitrate concentration increased by 50% near the ground when the heterogeneous hydrolysis of  $\text{N}_2\text{O}_5$  was accounted for, and the  $\text{HNO}_3$  mixing ratio increased by at most 40%, and 15% near the ground when comparing case B with case A.

[28] Including the effect of organics changes these findings in the following way: as shown in Figure 1, the presence of organics varied with height. Therefore the impact of the organic coating was not uniform over all heights. Figure 3 shows vertical profiles of the coating thickness  $\ell_i$  for the different modes, calculated on the basis of the median

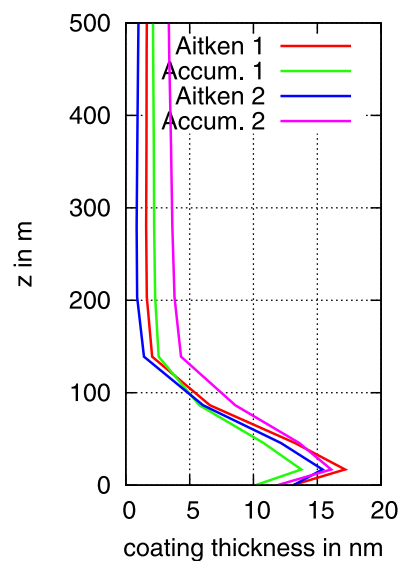


**Figure 3.** Vertical profiles of coating thickness for the two Aitken modes and the two accumulation modes at 0300 CET. The modes numbered with 1 refer to the soot-free modes; the modes numbered with 2 refer to the soot-containing modes.

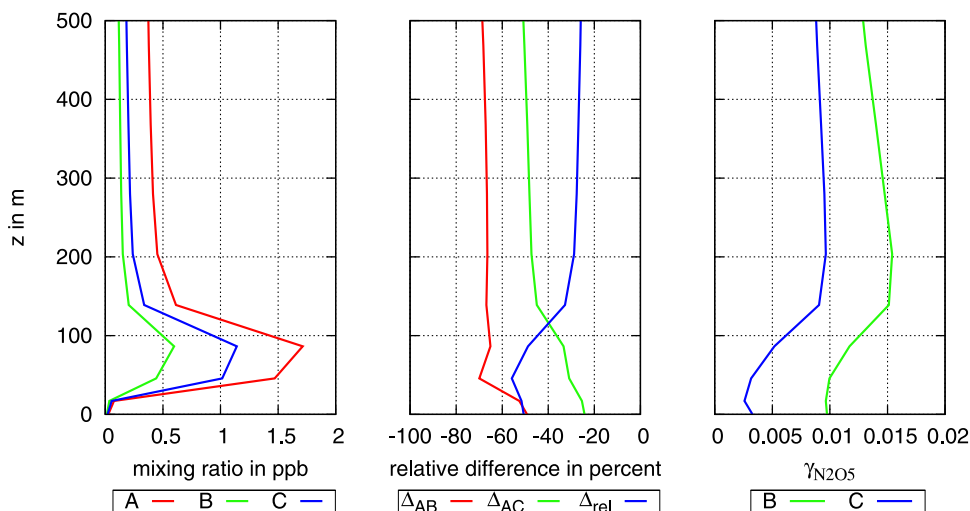


**Figure 4.** (left) Simulated profiles of the total of NO<sub>3</sub> and N<sub>2</sub>O<sub>5</sub>, TN = NO<sub>3</sub> + 2N<sub>2</sub>O<sub>5</sub> for the low-NO<sub>x</sub> conditions (cases A–C). (middle) Relative differences in TN depending on the parameterization of hydrolysis (see text for details). The blue curve gives the relative difference  $\Delta_{rel} = (\Delta_{AC} - \Delta_{AB})/\Delta_{AB}$  as a measure of the relative importance of the organic coating. (right) Simulated profiles of  $\gamma_{N_2O_5}$  for cases B and C.

diameter with respect to the surface area distribution for 0300 CET. The modes numbered with 1 refer to the soot-free modes, while the modes numbered with 2 refer to the soot-containing modes. For the different modes the values ranged between 14 and 17 nm in the lower part of the nocturnal boundary layer and decreased to values below 5 nm in the residual layer. Hence, as expected, the largest coatings were situated in the lower part of the nocturnal boundary layer.

[29] Figures 4–6 show vertical profiles of the total of NO<sub>3</sub> and N<sub>2</sub>O<sub>5</sub>, TN = NO<sub>3</sub> + 2N<sub>2</sub>O<sub>5</sub> to capture the net effect of varying the  $\gamma_{N_2O_5}$  parameterization on the NO<sub>y</sub> budget. Figure 4 displays the profiles of TN (Figure 4, left) and the relative differences (Figure 4, middle) for the low-NO<sub>x</sub> simulations: the red curve shows the vertical profile of the relative difference of TN mixing ratio for case A (TN<sub>A</sub>) and case B (TN<sub>B</sub>),  $\Delta_{AB} = (TN_B - TN_A)/TN_A$ . The green curve is the vertical profile of the relative difference in the TN mixing ratio between cases A and C (TN<sub>C</sub>),  $\Delta_{AC} = (TN_C - TN_A)/TN_A$ . While TN was reduced by 50% near the ground and up to 70% above 50 m in case B, the reduction was smaller for case C. This is expected since the formation of organic coatings lead to slower reactive uptake of N<sub>2</sub>O<sub>5</sub>. N<sub>2</sub>O<sub>5</sub> was reduced by only 25% near the ground, and up to 50% above 100 m in case C. This means that we encountered a relatively stronger impact of the organic coating near the ground, shown by the blue curve, which is the relative difference  $\Delta_{rel} = (\Delta_{AC} - \Delta_{AB})/\Delta_{AB}$ . This relative difference is equivalent to  $\Delta_{rel} = (TN_C - TN_B)/(TN_B - TN_A)$ , and assumes values between 0 and –100%. A value of  $\Delta_{rel}$  near 0 means that case B and case C are very similar, and hence the impact of the coating is relatively small. A value of  $\Delta_{rel}$  near –100% means that cases A and C are very similar, and hence the impact of the coating (in inhibiting the hydrolysis of N<sub>2</sub>O<sub>5</sub>) is relatively large. Figure 4 (right) shows the  $\gamma_{N_2O_5}$  values corresponding to cases B and C for the low-NO<sub>x</sub> case. For case B, the deviation of  $\gamma_{N_2O_5}$  from the value 0.02 reflects the presence of nitrate in the aerosol. This led to values of  $\gamma_{N_2O_5}$  of about 0.01 near the ground. For case C, the

$\gamma_{N_2O_5}$  values were additionally lowered by the presence of the organic coating, and this was most pronounced near the ground where values of  $\gamma_{N_2O_5} = 0.003$  occur.

[30] As pointed out above, we assumed so far that all SOA contributed to forming an organic coating. In a sensitivity run we explored how the results changed if we assumed that only a fraction of the organic material formed a coating and the rest dissolved in the core without affecting  $\gamma_{core}$ . Figure 5 illustrates the results assuming that 50% of the organic material contributed to the coating. Qualitatively this

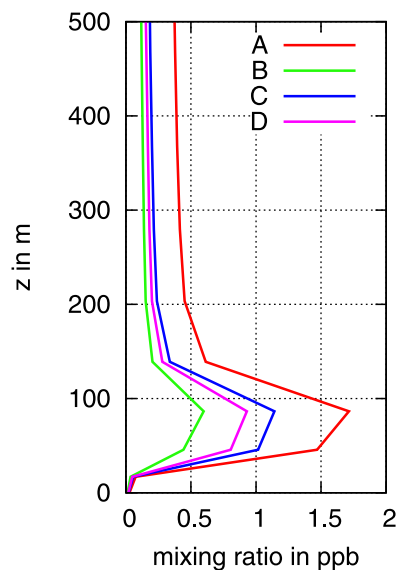


**Figure 5.** Simulated profiles of TN = NO<sub>3</sub> + 2N<sub>2</sub>O<sub>5</sub> for the low-NO<sub>x</sub> conditions, for the three different treatments of hydrolysis (cases A–C) and for an additional run assuming that only 50% of the organic material contributes to the coating (case D). The other 50% of the organic material is assumed to dissolve in the core.

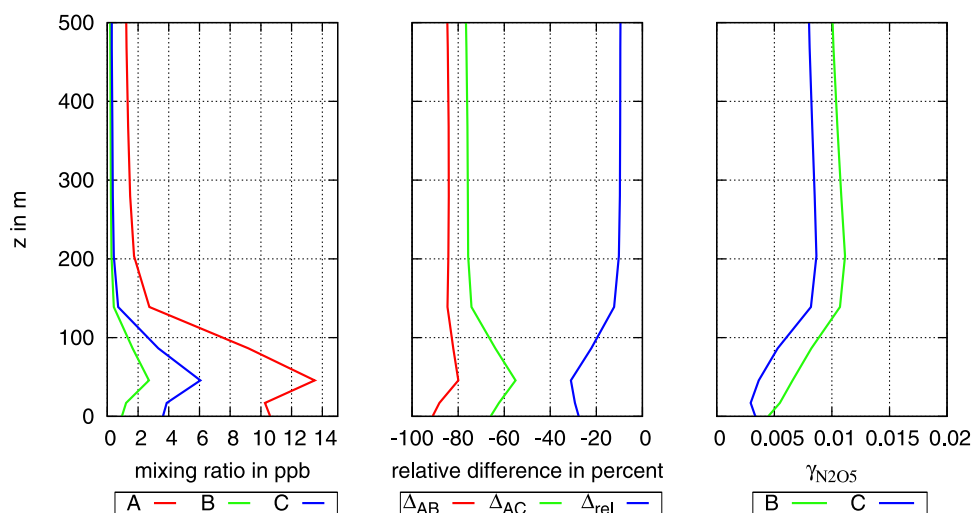


**Figure 6.** (left) Simulated profiles of  $TN = NO_3 + 2N_2O_5$  for the high- $NO_x$  conditions (cases A–C). (middle) Relative differences in TN depending on the parameterization of hydrolysis (see text for details). The blue curve gives the relative difference  $\Delta_{rel} = (\Delta_{AC} - \Delta_{AB})/\Delta_{AB}$  as a measure of the relative importance of the organic coating. (right) Simulated profiles of  $\gamma_{N_2O_5}$  for cases B and C.

case looks very similar to case C; however, the inhibition of hydrolysis was not as pronounced. The relative difference in the TN mixing ratio  $\Delta_{AD} = (TN_D - TN_A)/TN_A$  ranged between  $-33\%$  near the ground, and up to  $-60\%$  above 100 m.

[31] Last, we investigated the impact of organic coatings under conditions with higher  $NO_x$  emissions. For this purpose we multiplied the  $NO_x$  emissions by a factor of 10 compared to the standard case. This led to higher  $N_2O_5$  mixing ratios (3 ppb at 50 m height for case C), higher nitrate concentrations ( $40 \mu\text{g m}^{-3}$  near the ground for case C), but also a higher surface area ( $1500 \mu\text{m}^2 \text{cm}^{-3}$  near the ground for case C). Owing to the higher nitrate concentrations,  $\gamma_{core}$  was lowered, according to equation (5). Including the organic coating had an additionally decreasing effect on the overall reaction probability  $\gamma_{N_2O_5}$ ; however, its relative impact,  $\Delta_{rel}$ , was smaller than in the situation with low- $NO_x$  emissions, as shown in Figure 6 (middle). This is consistent with findings by T. F. Mentel et al. (unpublished report, 2000), who showed in their laboratory studies that the organic coating effect is small for nitrate-containing aerosols. This result can be understood on the basis of the resistor formalism (equation (4)): the addition of an organic coating to an aqueous particle has a larger effect on the reactive uptake rate when the heterogeneous hydrolysis of  $N_2O_5$  proceeds more rapidly in the aqueous phase. The  $\gamma_{N_2O_5}$  profiles in Figure 6 (right) show that for case B,  $\gamma_{N_2O_5}$  values of 0.005 occurred near the ground, reflecting a nitrate content of about 85%. The  $\gamma_{N_2O_5}$  values for case C were still lower than in case B, but the difference was not as pronounced as in the low- $NO_x$  case. Hence we conclude that the relative impact of the organic coating depends on the nitrate content of the inorganic core. We explore this issue further for the results of the three-dimensional simulations in section 4.

[32] In summary, the one-dimensional model simulations showed that nighttime oxidation of VOCs may lead, through gas-particle partitioning of low-volatility oxidation products,

to the formation of organic coatings that are thick enough to suppress the reactive uptake of  $N_2O_5$  by aqueous particles. Under certain conditions, this was demonstrated to have a notable impact on the ambient mixing ratios of nitrogen oxides. The magnitude of the impact was further shown to depend on the altitude, degree of the pollution (in terms of the  $NO_x$  mixing ratio levels) and on the physicochemical properties of the organic coatings. These results thus motivate the use of three-dimensional model simulations, which are discussed next.

#### 4. Three-Dimensional Simulations

[33] As a next step we carried out three-dimensional simulations to investigate the impact of the organic coating in a more realistic setting. In addition to vertical mixing, these simulations included horizontal transport processes and a spatially varying emission distribution, which resulted in regions with different photochemical regimes. Moreover, the meteorological conditions were highly variable, which influenced the biogenic VOC emissions. We focused on a situation in summer to allow higher biogenic emissions and therefore higher secondary organic aerosol formation.

[34] We used the model system COSMO-ART. COSMO (formerly Lokalmodell) is a nonhydrostatic mesoscale model and is part of the forecast system of the German Weather Service (DWD). ART stands for Aerosol and Reactive Trace gases and includes the modules RADMKA for gas phase reactions and MADEsoot for aerosol dynamics and chemistry, which are described in section 3. To calculate the photolysis rates we used a new scheme, which is described in detail by Vogel et al. [2009]. The biogenic VOC emissions were calculated on the basis of the land use using the Global Land Cover 2000 data set provided by the Joint Research Center at Ispra (<http://www-tem.jrc.it/glc2000/>), the modeled temperatures, and modeled radiative fluxes [Vogel et al., 1995]. We did not use the recent model extension to include emissions of dust and sea salt particles.

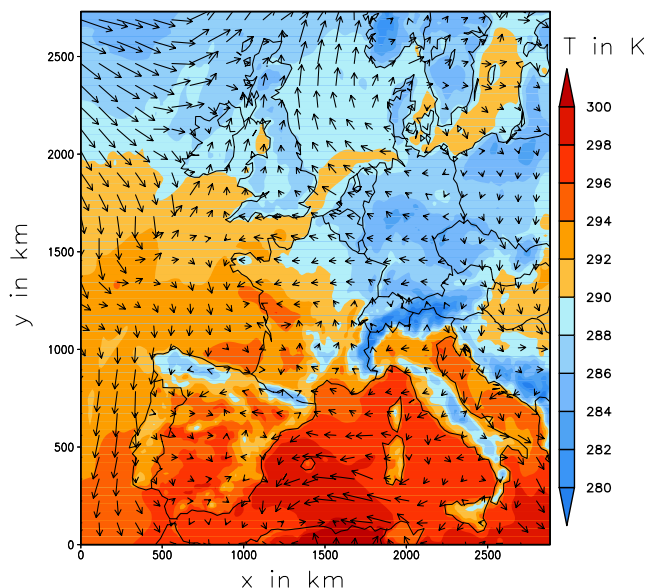


**Figure 7.** Simulated wind and temperature fields on 18 August 2005 at 0200 UTC, 20 m above ground.

Mineral dust resides mainly in the coarse mode, which does not supply much surface area. We therefore do not expect that our conclusions will change much because of the omission of mineral dust. Sea salt is present in the coarse mode and in the accumulation mode, and it is a common aerosol type in the coastal areas. Therefore we cannot exclude the possibility that our results would change somewhat in these regions if sea salt were included.

[35] The whole model system ran in a fully coupled model. For our study we simulated a typical summer period from 16–20 August 2005. Simulations were performed over Europe with a horizontal grid size of 14 km. We allowed for a 2-day spin-up time of the model. A total of 40 vertical layers were considered with a vertical grid size

of about 20 m close to the ground up to 2000 m at the top of the model domain at 20 km above sea level. The time step was 40 s. We used background concentrations for the gaseous and particulate matter at the lateral boundaries.

[36] The anthropogenic emissions of the gases SO<sub>2</sub>, CO, NO<sub>x</sub>, NH<sub>3</sub>, and 32 individual classes of VOC, and of the particle classes PM<sub>10</sub>, PM<sub>2.5</sub>, PM<sub>1</sub>, EC<sub>10</sub>, EC<sub>2.5</sub>, and EC<sub>1</sub>, were precalculated with a spatial resolution of 14 × 14 km<sup>2</sup>. The temporal resolution of the emission data was 1 h. We had no data available for the primary emissions of organic compounds. The anthropogenic emission data accounted for traffic emissions, emissions by large point sources, and area sources such as households and industrial areas. The method used to determine these emissions is described by *Pregger et al.* [2007]. The formation of organic coatings and their effect on heterogeneous N<sub>2</sub>O<sub>5</sub> hydrolysis were considered as described in detail in section 2.2. For the calculation of the surface area, cloud and fog droplets were not taken into account.

[37] At the beginning of the episode the meteorological situation was characterized by a high-pressure ridge over France and Great Britain. During the following days the system moved to the East and a weak low-pressure system over the southwest of Europe developed. Consequently, easterly wind conditions were prevailing over Central Europe during 16 and 17 August 2005. On 18 August the wind direction changed to the west over France. As for the one-dimensional studies, we carried out three simulations. Case A was the simulation without the hydrolysis of N<sub>2</sub>O<sub>5</sub>, case B included hydrolysis, and case C took into account the effect of the organic coating. In the following we focus on the comparisons of results for cases B and C.

[38] Figure 7 shows the horizontal distribution of the temperature and the wind vectors close to the surface on 18 August 2005 at 0200 UTC. Figure 8 shows the corresponding horizontal distribution of N<sub>2</sub>O<sub>5</sub> (Figure 8, left) and the secondary organic mass in the aerosol (Figure 8, right) for case C at the same point in time. The highest N<sub>2</sub>O<sub>5</sub>

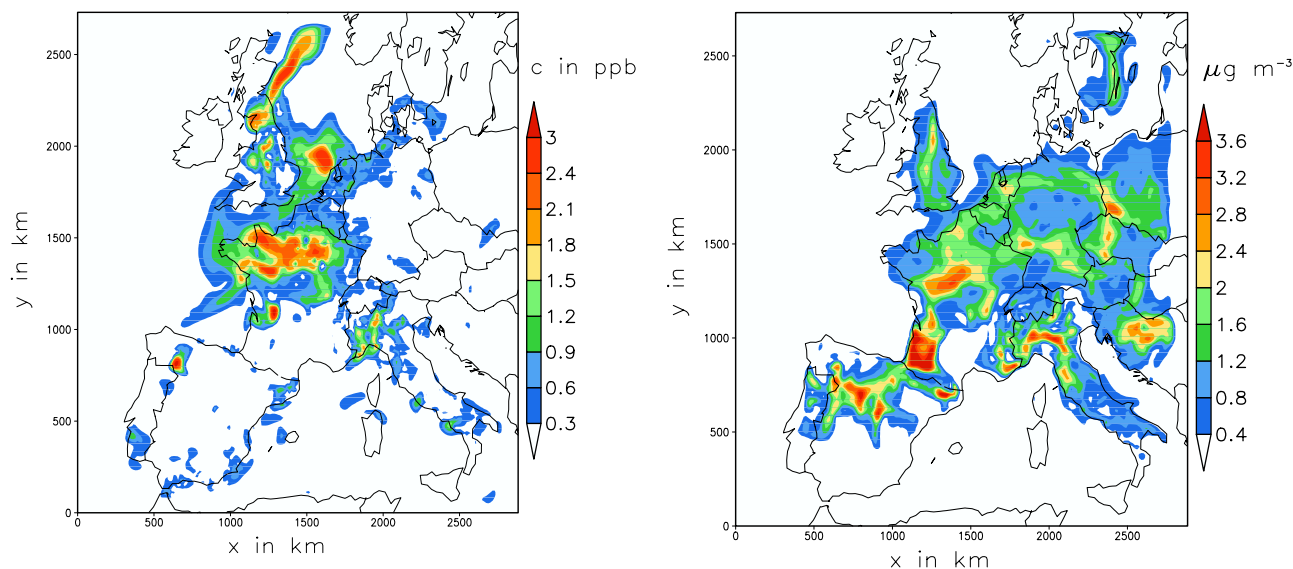


**Figure 8.** Simulated (left) N<sub>2</sub>O<sub>5</sub> mixing ratio and (right) organic mass concentration in the aerosol for case C on 18 August 2005 at 0200 UTC, 20 m above ground.

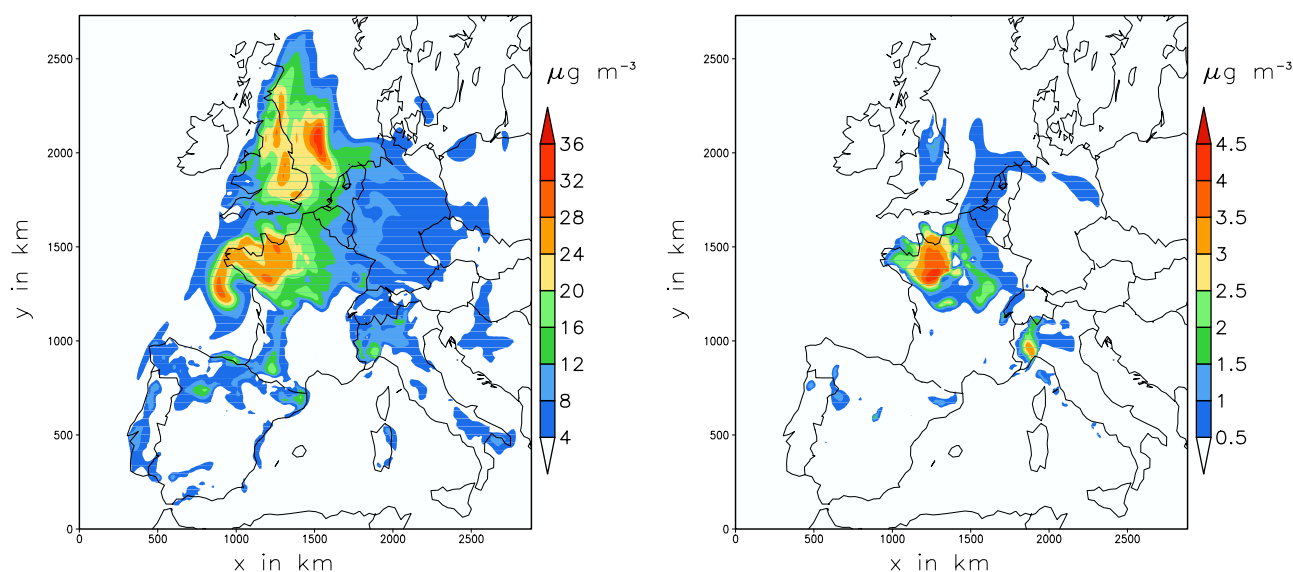


**Figure 9.** (left) Simulated nitrate concentration for case B and (right) the nitrate difference between cases B and C on 18 August 2005 at 0800 UTC, 20 m above ground.

mixing ratios occurred over northern France, the Po Valley and in two plumes over the North Sea. The situation was different for secondary organic aerosol mass. The highest SOA concentrations were simulated over Spain, in the southwestern part of France and the northern part of Italy. The nitrate concentration for case B and the differences between the simulations B and C ( $\Delta\text{NO}_3^-$ ) are shown in Figure 9 at 0800 UTC. The maximum of  $\Delta\text{NO}_3^-$  appeared over northwest France and in the Po Valley, an area where large absolute nitrate concentrations also existed. In these areas the nitrate concentration was about 15–30% lower for case C than for case B. This was caused by favorable temperature conditions (compare Figure 7) for biogenic emissions as well as for the formation of SOA.

[39] About 24 h later the situation was quite different. The low-pressure system had its center over the North Sea north of France with the corresponding wind field shown in Figure 10. Figure 11 shows the N<sub>2</sub>O<sub>5</sub> mixing ratios (Figure 11, left) and SOA (Figure 11, right) concentrations for 19 August 2005 at 0200 UTC. Again, rather high concentrations of N<sub>2</sub>O<sub>5</sub> and SOA were simulated in the Po Valley, and also in the region of the low-pressure system over northern France, Belgium and western Germany. In those parts of the model system the prerequisites for an influence of the organic coating on hydrolysis were achieved. We find differences in the nitrate concentrations of up to about 4.5  $\mu\text{g m}^{-3}$ . This corresponds to a change of about 10% (Figure 12). The simulations show that during a specific episode the conditions for the formation of N<sub>2</sub>O<sub>5</sub> and SOA are very variable. In the parts of the model domain where both components build up, the impact of an organic coating on the hydrolysis of N<sub>2</sub>O<sub>5</sub> can decrease the nitrate concentrations by up to 20%. If these prerequisites are not fulfilled then the impact is negligible.

[40] As mentioned in section 3, the one-dimensional simulations suggest that the importance of the organic coating depends on the nitrate content. Figure 13 shows how this finding applies to the 3-D simulations. We quantified the

relative importance of the organic coating on nitrate by considering the relative difference between the nitrate concentrations in cases B and C:  $\Delta_{BC} = (\text{NO}_3^- (\text{B}) - \text{NO}_3^- (\text{C})) / \text{NO}_3^- (\text{B})$ . Figure 13 displays  $\Delta_{BC}$  versus the nitrate concentration for case B for all grid points in the first layer above the surface at the time when  $\Delta_{BC}$  reaches its overall maximum in the model domain. Data points in red and blue correspond to 19 and 20 August, respectively. Only when the nitrate concentration exceeded a threshold of 1  $\mu\text{g m}^{-3}$  was the data point included in Figure 13. For both days the data points from the entire model domain follow a certain universal relationship. The relative differences between cases B and C reached values of up to 90% when the nitrate concentrations

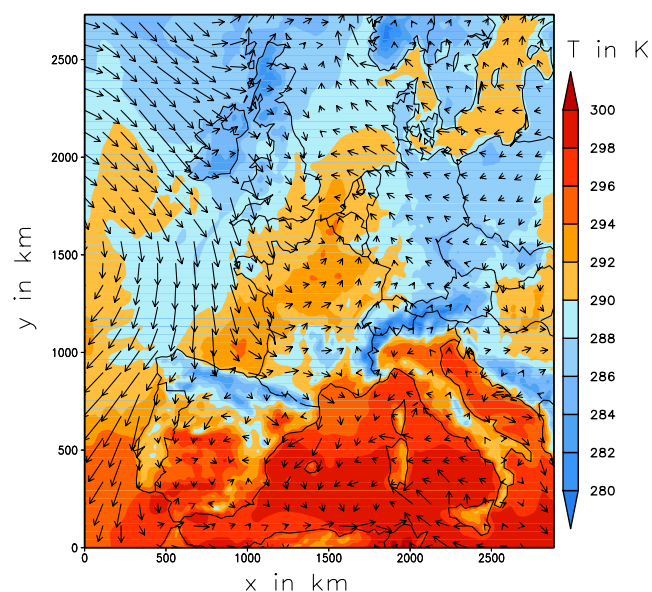


**Figure 10.** Simulated wind and temperature fields on 19 August 2005 at 0200 UTC, 20 m above ground.

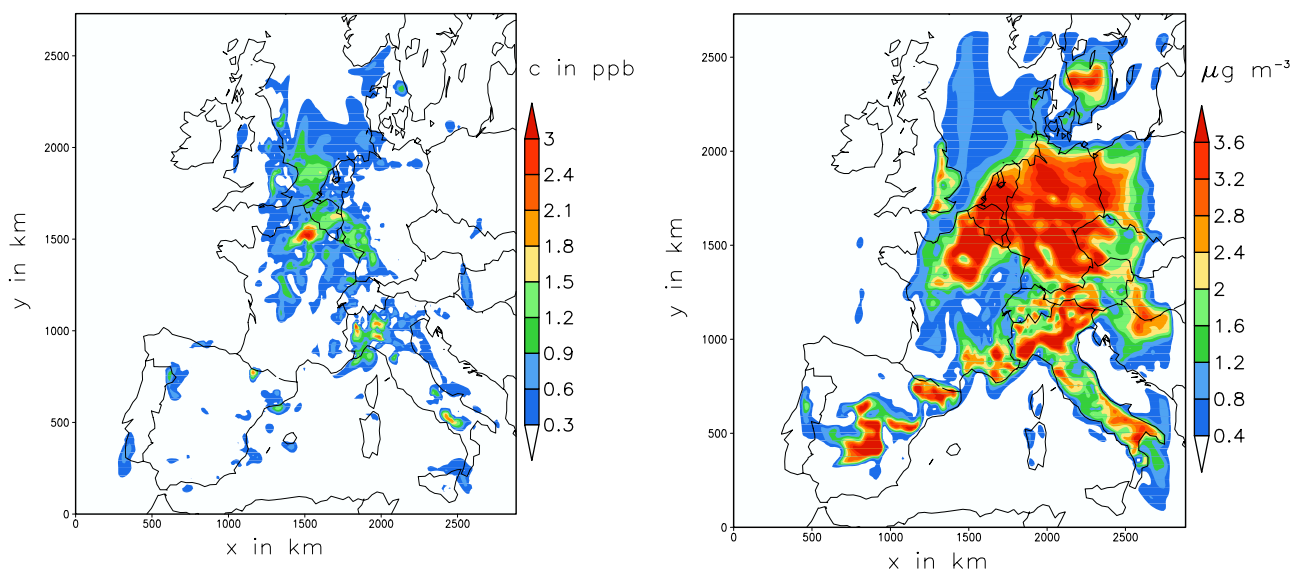


**Figure 11.** Simulated (left) N<sub>2</sub>O<sub>5</sub> mixing ratio and (right) organic mass concentration in the aerosol for case C on 19 August 2005 at 0200 UTC, 20 m above ground.

were low. This means that under low-nitrate conditions, the relative importance of an organic coating is high. As the nitrate concentration increased, that is, when the nitrate effect already suppressed hydrolysis,  $\Delta_{BC}$  decreased to about 10%. It should be noted that, as recent work by *Davis et al.* [2008] suggests, equation (5) may overestimate the nitrate effect. Moreover, the current state-of-the-art model treatment of SOA formation has large uncertainties by itself. In particular, several recent studies have shown that current models significantly underpredict SOA formation in the ambient urban atmosphere as well as in the upper troposphere [*de Gouw et al.*, 2005; *Heald et al.*, 2005; *Johnson et al.*, 2006; *Volkamer et al.*, 2006]. Hence the importance of

organic coatings may be larger than indicated in the present study.

## 5. Conclusions

[41] With this study we investigated how a decrease in  $\gamma_{N_2O_5}$  due to the presence of nitrate or organic coatings influences the chemistry in the ambient atmosphere. To treat N<sub>2</sub>O<sub>5</sub> hydrolysis, we built on our previous study [*Riemer et al.*, 2003b] and used recent results from laboratory experiments that quantify  $\gamma_{N_2O_5}$  on the basis of the organic coating thickness [*Anttila et al.*, 2007; T. F. Mentel et al., unpublished report, 2005]. We assumed that all the organic material contributed to the coating, and hence the results represent

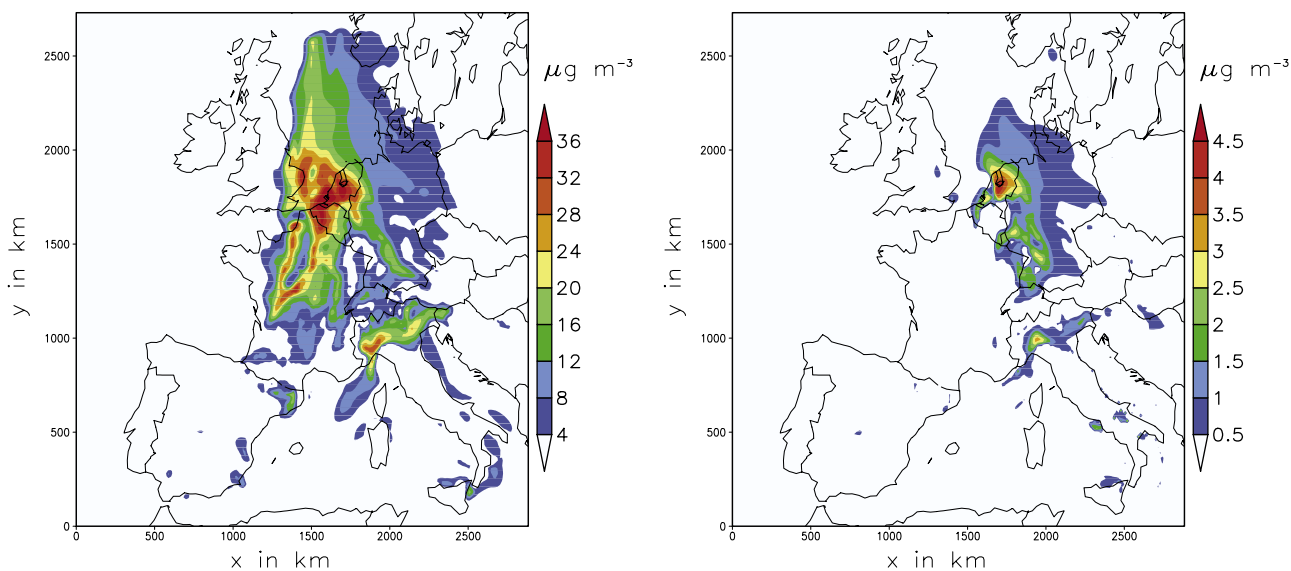


**Figure 12.** (left) Simulated nitrate concentration for case B and (right) the nitrate difference between cases B and C on 19 August 2005 at 1000 UTC, 20 m above ground.

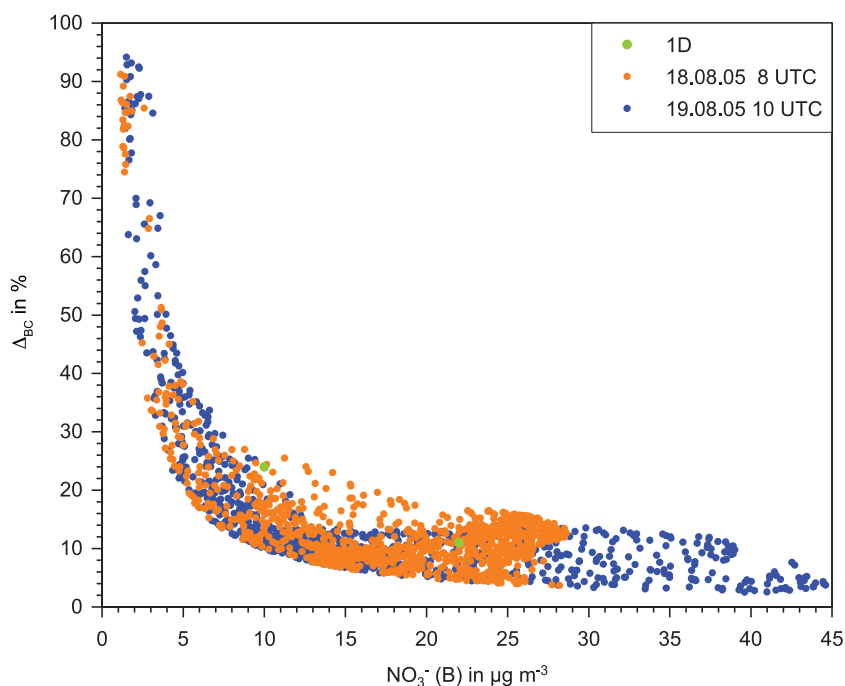


**Figure 13.** Relative nitrate difference in percent between cases B and C versus nitrate concentration of case B on 18 and 19 August 2005 at 1000 UTC, 20 m above ground. The green dots show the results of the two one-dimensional simulations with low- and high-NO<sub>x</sub> emissions.

an upper estimate. We presented results of one-dimensional process studies and three-dimensional regional-scale model simulations during summer for Europe with the comprehensive model system COSMO-ART.

[42] Comparing the results of sensitivity runs with the one-dimensional model we draw the following conclusions:

[43] 1. Independent of the treatment of the hydrolysis reaction, aerosol and gas phase species involved in N<sub>2</sub>O<sub>5</sub> hydrolysis exhibited characteristic profiles within the stable nocturnal boundary layer with strong vertical gradients (see the profiles of N<sub>2</sub>O<sub>5</sub> and nitrate as an example in Figure 1). These profiles were the result of chemical production and loss processes combined with weak turbulent diffusion. Resolving these profiles adequately is a prerequisite for a good representation of the N<sub>2</sub>O<sub>5</sub> hydrolysis and poses an important modeling challenge.

[44] 2. By comparing the one-dimensional sensitivity cases A, B, and C shown in Figure 1, we found that organic coatings can effectively suppress N<sub>2</sub>O<sub>5</sub> heterogeneous hydrolysis. We found an impact on nighttime mixing ratios of N<sub>2</sub>O<sub>5</sub>, NO<sub>3</sub>, nitrate, and VOC.

[45] 3. The relative impact of the organic coating was maximal near the ground where, in our simulations, the highest SOA mass resided. If the aerosol contained nitrate, the relative importance of the organic coating decreased.

[46] While the one-dimensional simulations were instructive to identify the individual processes, three-dimensional simulations with COSMO-ART were carried out to obtain a more realistic picture of the impact of the organic coating on the regional scale. Simulations were performed for the episode of 16–20 August 2005. For the organic coating to have an impact, both N<sub>2</sub>O<sub>5</sub> and SOA needed to be present at the same location. The results showed that this condition was only sometimes fulfilled and that there were large

variations from day to day caused by changing meteorological conditions. In parts of the model domain where both components were present, the impact of an organic coating on the hydrolysis of N<sub>2</sub>O<sub>5</sub> decreased the maximum nitrate concentrations by up to 20%. Analyzing the relative importance ( $\Delta_{BC}$ ) of the organic coating for the nitrate concentration, we found a relationship between  $\Delta_{BC}$  and the amount of nitrate in the aerosol. When the nitrate levels were low,  $\Delta_{BC}$  reached values of up to 90%. For nitrate concentrations above 15  $\mu\text{g m}^{-3}$ ,  $\Delta_{BC}$  decreased down to 10–15%. This relationship appeared to hold for both days. It suggests that the organic coating effect on N<sub>2</sub>O<sub>5</sub> hydrolysis is particularly important and should be included in model simulations when low-nitrate concentrations are expected. Under conditions with high-nitrate concentrations the relative impact of the organic coating decreases. While some field observations [Brown *et al.*, 2006] show reduced uptake accompanying enhanced organic fractions, these findings remain to be confirmed by field observations.

## References

- Adrian, G., and F. Fiedler (1991), Simulation of unstationary wind and temperature fields over complex terrain and comparison with observations, *Contrib. Atmos. Phys.*, *64*, 27–48.
- Anttila, T., A. Kiendler-Scharr, R. Tillmann, and T. F. Mentel (2006), On the reactive uptake of gaseous compounds by organic-coated aqueous aerosols: Theoretical analysis and application to the heterogeneous hydrolysis of N<sub>2</sub>O<sub>5</sub>, *J. Phys. Chem. A*, *110*, 10,435–10,443, doi:10.1021/jp062403c.
- Anttila, T., A. Kiendler-Scharr, T. F. Mentel, and R. Tillmann (2007), Size dependent partitioning of organic material: Evidence for the formation of organic coatings on aqueous aerosols, *J. Atmos. Chem.*, *57*, 215–237, doi:10.1007/s10874-007-9067-9.
- Badger, C. L., P. T. Griffiths, I. George, J. P. D. Abbatt, and R. A. Cox (2006), Reactive uptake of (N<sub>2</sub>O<sub>5</sub>) by aerosol particles containing mixtures of humic acid and ammonium sulfate, *J. Phys. Chem. A*, *110*, 6986–6994, doi:10.1021/jp0562678.

- Bär, M., and K. Nester (1992), Parameterization of trace gas dry deposition velocities for a regional mesoscale diffusion model, *Ann. Geophys.*, *10*, 912–923.
- Binkowski, F. S., and U. Shankar (1995), The Regional Particulate Matter Model: 1. Model description and preliminary results, *J. Geophys. Res.*, *100*(D12), 26,191–26,209, doi:10.1029/95JD02093.
- Bohn, B., and C. Zetzsch (1997), Rate constants of HO<sub>2</sub> + NO covering atmospheric conditions: 1. HO<sub>2</sub> formed by OH + H<sub>2</sub>O<sub>2</sub>, *J. Phys. Chem.*, *101*, 1488–1493.
- Brown, S. S., et al. (2004), Nighttime removal of NO<sub>x</sub> in the summer marine boundary layer, *Geophys. Res. Lett.*, *31*, L07108, doi:10.1029/2004GL019412.
- Brown, S. S., et al. (2006), Variability in nocturnal nitrogen oxide processing and its role in regional air quality, *Science*, *311*, 67–70, doi:10.1126/science.1120120.
- Brown, S. S., W. P. Dube, H. D. Osthoff, D. E. Wolfe, W. M. Angevine, and A. R. Ravishankara (2007a), High resolution vertical distributions of NO<sub>3</sub> and N<sub>2</sub>O<sub>5</sub> through the nocturnal boundary layer, *Atmos. Chem. Phys.*, *7*, 139–149.
- Brown, S. S., et al. (2007b), Vertical profiles in NO<sub>3</sub> and N<sub>2</sub>O<sub>5</sub> measured from an aircraft: Results from the NOAA P-3 and surface platforms during the New England Air Quality Study 2004, *J. Geophys. Res.*, *112*, D22304, doi:10.1029/2007JD008883.
- Cosman, L. M., D. A. Knopf, and A. K. Bertram (2008), N<sub>2</sub>O<sub>5</sub> reactive uptake on aqueous sulfuric acid solutions coated with branched and straight-chain insoluble organic surfactants, *J. Phys. Chem. A*, *112*, 2386–2396, doi:10.1021/jp710685r.
- Davis, J. M., P. V. Bhavsar, and K. M. Foley (2008), Parameterization of N<sub>2</sub>O<sub>5</sub> reaction probabilities on the surface of particles containing ammonium, sulfate, and nitrate, *Atmos. Chem. Phys.*, *8*, 5295–5311.
- de Gouw, J. A., et al. (2005), The budget of organic carbon in a polluted atmosphere: Results from the New England Air Quality Study in 2002, *J. Geophys. Res.*, *110*, D16305, doi:10.1029/2004JD005623.
- Dentener, F. J., and P. J. Crutzen (1993), Reaction of N<sub>2</sub>O<sub>5</sub> on tropospheric aerosols: Impact on the global distribution of NO<sub>x</sub>, O<sub>3</sub>, and OH, *J. Geophys. Res.*, *98*(D4), 7149–7163, doi:10.1029/92JD02979.
- Donahue, N. M., M. K. Dubey, R. Mohrschladt, K. L. Demerjian, and J. G. Anderson (1997), High pressure flow study of the reactions OH + NO<sub>x</sub> → HONO<sub>x</sub>: Errors in the falloff region, *J. Geophys. Res.*, *102*(D5), 6159–6168, doi:10.1029/96JD02329.
- Ellison, G. B., A. F. Tuck, and V. Vaida (1999), Atmospheric processing of organic aerosols, *J. Geophys. Res.*, *104*(D9), 11,633–11,641, doi:10.1029/1999JD900073.
- Evans, M. J., and D. J. Jacob (2005), Impact of new laboratory studies of N<sub>2</sub>O<sub>5</sub> hydrolysis on global model budgets of tropospheric nitrogen oxides, ozone, and OH, *Geophys. Res. Lett.*, *32*, L09813, doi:10.1029/2005GL022469.
- Folkers, M., T. F. Mentel, and A. Wahner (2003), Influence of an organic coating on the reactivity of aqueous aerosols probed by the heterogeneous hydrolysis of N<sub>2</sub>O<sub>5</sub>, *Geophys. Res. Lett.*, *30*(12), 1644, doi:10.1029/2003GL017168.
- Geiger, H., I. Barnes, I. Bejan, T. Benter, and M. Spittler (2003), The tropospheric degradation of isoprene: An updated module for the regional atmospheric chemistry mechanism, *Atmos. Environ.*, *37*, 1503–1519, doi:10.1016/S1352-2310(02)01047-6.
- Geyer, A., and J. Stutz (2004), Vertical profiles of NO<sub>3</sub>, N<sub>2</sub>O<sub>5</sub>, O<sub>3</sub>, and NO<sub>x</sub> in the nocturnal boundary layer: 2. Model studies on the altitude dependence of composition and chemistry, *J. Geophys. Res.*, *109*, D12307, doi:10.1029/2003JD004211.
- Gill, P. S., T. E. Graedel, and C. J. Weschler (1983), Organic films on atmospheric particles, fog droplets, cloud droplets, raindrops, and snowflakes, *Rev. Geophys.*, *21*, 903–920, doi:10.1029/RG021i004p00903.
- Hanson, D. R., A. R. Ravishankara, and S. Solomon (1994), Heterogeneous reactions in sulfuric acid aerosols: A framework for model calculations, *J. Geophys. Res.*, *99*(D2), 3615–3629, doi:10.1029/93JD02932.
- Heald, C. L., D. J. Jacob, R. J. Park, L. M. Russell, B. J. Huebert, J. H. Seinfeld, H. Liao, and R. J. Weber (2005), A large organic aerosol source in the free troposphere missing from current models, *Geophys. Res. Lett.*, *32*, L18809, doi:10.1029/2005GL023831.
- Jacob, D. J. (2000), Heterogeneous chemistry and tropospheric ozone, *Atmos. Environ.*, *34*, 2131–2159, doi:10.1016/S1352-2310(99)00462-8.
- Johnson, D., S. R. Utembe, M. E. Jenkin, R. G. Derwent, G. D. Hayman, M. R. Alfarra, H. Coe, and G. McFiggans (2006), Simulating regional scale secondary organic aerosol formation during the TORCH 2003 campaign in the southern UK, *Atmos. Chem. Phys.*, *6*, 403–418.
- McNeill, V. M., J. Patterson, M. Wolfe, and J. A. Thornton (2006), The effect of varying levels of surfactant on the reactive uptake of (N<sub>2</sub>O<sub>5</sub>) to aqueous aerosol, *Atmos. Chem. Phys.*, *6*, 1635–1644.
- Mentel, T. F., M. Sohn, and A. Wahner (1999), Nitrate effect in the heterogeneous hydrolysis of dinitrogen pentoxide on aqueous aerosols, *Phys. Chem. Chem. Phys.*, *1*, 5451–5457.
- Mihelcic, D., D. Klemp, P. Müsgen, H. W. Pätz, and A. Volz-Thomas (1993), Simultaneous measurements of peroxy and nitrate radicals at Schauinsland, *J. Atmos. Chem.*, *16*, 313–335, doi:10.1007/BF01032628.
- Mochida, M., Y. Kitamori, and K. Kawamura (2002), Fatty acids in the marine atmosphere: Factors governing their concentrations and evaluation of organic films on sea-salt particles, *J. Geophys. Res.*, *107*(D17), 4325, doi:10.1029/2001JD001278.
- Mozurkewich, M., and J. G. Calvert (1988), Reaction probability of N<sub>2</sub>O<sub>5</sub> on aqueous aerosols, *J. Geophys. Res.*, *93*(D12), 15,889–15,896, doi:10.1029/JD093iD12p15889.
- Odum, J. R., T. Hoffmann, F. Bowman, D. Collins, R. C. Flagan, and J. H. Seinfeld (1996), Gas/particle partitioning and secondary organic aerosol yields, *Environ. Sci. Technol.*, *30*, 2580–2585, doi:10.1021/es950943+.
- Platt, U. F., A. M. Winer, H. W. Biermann, R. Atkinson, and J. N. Pitts Jr. (1984), Measurement of nitrate radical concentrations in continental air, *Environ. Sci. Technol.*, *18*, 365–369, doi:10.1021/es00123a015.
- Platt, U. F., G. Le Bras, G. Poulet, J. P. Burrows, and G. K. Moortgat (1990), Peroxy radicals from nighttime reaction of NO<sub>3</sub> with organic compounds, *Nature*, *348*, 147–149, doi:10.1038/348147a0.
- Pöschl, U., Y. Rudich, and M. Ammann (2007), Kinetic model framework for aerosol and cloud surface chemistry and gas-particle interactions—Part 1: General equations, parameters, and terminology, *Atmos. Chem. Phys.*, *7*, 5989–6023.
- Pregger, T., B. Thiruchittampalam, and R. Friedrich (2007), Ermittlung von Emissionsdaten zur Untersuchung der Klimawirksamkeit von Rußpartikeln in Baden-Württemberg, final report, Inst. für Energiewirt. und Rationelle Energieanwendung, Univ. Stuttgart, Stuttgart, Germany.
- Ravishankara, A. R., and C. Longfellow (1999), Reactions on tropospheric condensed matter, *Phys. Chem. Chem. Phys.*, *1*, 5433–5441, doi:10.1039/a905660b.
- Riemer, N., H. Vogel, B. Vogel, and F. Fiedler (2003a), Modeling aerosols on the mesoscale-γ: Treatment of soot aerosol and its radiative effects, *J. Geophys. Res.*, *108*(D19), 4601, doi:10.1029/2003JD003448.
- Riemer, N., H. Vogel, B. Vogel, B. Schell, I. Ackermann, C. Kessler, and H. Hass (2003b), Impact of the heterogeneous hydrolysis of N<sub>2</sub>O<sub>5</sub> on chemistry and nitrate aerosol formation in the lower troposphere under photosmog conditions, *J. Geophys. Res.*, *108*(D4), 4144, doi:10.1029/2002JD002436.
- Russell, L. M., S. F. Maria, and S. C. B. Myneni (2002), Mapping organic coatings on atmospheric particles, *Geophys. Res. Lett.*, *29*(16), 1779, doi:10.1029/2002GL014874.
- Saathoff, H., K. H. Naumann, M. Schnaiter, W. Schöck, O. Möhler, U. Schurath, E. Weingartner, M. Gysel, and U. Baltensperger (2003), Coating of soot and (NH<sub>4</sub>)<sub>2</sub>SO<sub>4</sub> particles by ozonolysis products of α-pinene, *J. Aerosol Sci.*, *34*(10), 1297–1321, doi:10.1016/S0021-8502(03)00364-1.
- Schell, B., I. J. Ackermann, H. Hass, F. S. Binkowski, and A. Ebel (2001), Modeling the formation of secondary organic aerosol within a comprehensive air quality model system, *J. Geophys. Res.*, *106*(D22), 28,275–28,293, doi:10.1029/2001JD000384.
- Smoydzin, L., and R. von Glasow (2007), Do organic surface films on sea salt aerosols influence atmospheric chemistry?—A model study, *Atmos. Chem. Phys.*, *7*, 5555–5567.
- Stockwell, W., P. Middleton, J. Chang, and X. Tang (1990), The second generation regional acid deposition model chemical mechanism for regional air quality modeling, *J. Geophys. Res.*, *95*, 16,343–16,367.
- Stutz, J., B. Alicke, R. Ackermann, A. Geyer, A. White, and E. Williams (2004), Vertical profiles of NO<sub>3</sub>, N<sub>2</sub>O<sub>5</sub>, O<sub>3</sub>, and NO<sub>x</sub> in the nocturnal boundary layer: 1. Observations during the Texas Air Quality Study 2000, *J. Geophys. Res.*, *109*, D12306, doi:10.1029/2003JD004209.
- Tervahattu, H., K. Hartonen, V.-M. Kerminen, K. Kupiainen, P. Aarnio, T. Koskentalo, A. F. Tuck, and V. Vaida (2002a), New evidence of an organic layer on marine aerosols, *J. Geophys. Res.*, *107*(D7), 4053, doi:10.1029/2000JD000282.
- Tervahattu, H., J. Juhanaja, and K. Kupiainen (2002b), Identification of an organic coating on marine aerosol particles by TOF-SIMS, *J. Geophys. Res.*, *107*(D16), 4319, doi:10.1029/2001JD001403.
- Tervahattu, H., J. Juhanaja, V. Vaida, A. F. Tuck, J. V. Niemi, K. Kupiainen, M. Kulmala, and H. Vehkamäki (2005), Fatty acids on continental sulphate aerosol particles, *J. Geophys. Res.*, *110*, D06207, doi:10.1029/2004JD005400.
- Thornton, J. A., and J. P. D. Abbatt (2005), N<sub>2</sub>O<sub>5</sub> reaction on submicron sea salt aerosol: Kinetics, products, and the effect of surface active organics, *J. Phys. Chem. A*, *109*, 10,004–10,012, doi:10.1021/jp054183t.
- Thornton, J. A., C. F. Braban, and J. P. D. Abbatt (2003), N<sub>2</sub>O<sub>5</sub> hydrolysis on sub-micron organic aerosols: The effect of relative humidity, particle phase, and particle size, *Phys. Chem. Chem. Phys.*, *5*, 4593–4603, doi:10.1039/b307498f.

- Tuazon, E. C., R. Atkinson, C. N. Plum, A. M. Winer, and J. N. Pitts Jr. (1983), The reaction of gas phase N<sub>2</sub>O<sub>5</sub> with water vapor, *Geophys. Res. Lett.*, *10*, 953–956, doi:10.1029/GL010i010p00953.
- Varutbangkul, V., F. J. Brechtel, R. Bahreini, N. L. Ng, M. D. Keywood, J. H. Kroll, R. C. Flagan, J. H. Seinfeld, A. Lee, and A. H. Goldstein (2006), Hygroscopicity of secondary organic aerosols formed by oxidation of cycloalkenes, monoterpenes, sesquiterpenes, and related compounds, *Atmos. Chem. Phys.*, *6*, 2367–2388.
- Vogel, B., F. Fiedler, and H. Vogel (1995), Influence of topography and biogenic volatile organic compounds emission in the state of Baden-Württemberg on ozone concentrations during episodes of high air temperatures, *J. Geophys. Res.*, *100*, 22,907–22,928, doi:10.1029/95JD01228.
- Vogel, B., H. Vogel, J. Kleffmann, and R. Kurtenbach (2003), Measured and simulated vertical profiles of nitrous acid, Part II—Model simulations and indications for a photolytic source, *Atmos. Environ.*, *37*, 2957–2966, doi:10.1016/S1352-2310(03)00243-7.
- Vogel, B., H. Vogel, D. Bäumer, M. Bangert, K. Lundgren, R. Rinke, and T. Stanelle (2009), The comprehensive model system COSMO-ART: Radiative impact of aerosol on the state of the atmosphere on the regional scale, *Atmos. Chem. Phys. Discuss.*, *9*, 14,483–14,528.
- Vogel, H., A. Pauling, and B. Vogel (2008), Numerical simulation of birch pollen dispersion with an operational weather forecast system, *Int. J. Biometeorol.*, *52*, 805–814, doi:10.1007/s00484-008-0174-3.
- Volkamer, R., J. L. Jimenez, F. San Martini, K. Dzepina, Q. Zhang, D. Salcedo, L. T. Molina, D. R. Worsnop, and M. J. Molina (2006), Secondary organic aerosol formation from anthropogenic air pollution: Rapid and higher than expected, *Geophys. Res. Lett.*, *33*, L17811, doi:10.1029/2006GL026899.
- Wahner, A., T. F. Mentel, and M. Sohn (1998a), Gas-phase reaction of N<sub>2</sub>O<sub>5</sub> with water vapor: Importance of heterogeneous hydrolysis of N<sub>2</sub>O<sub>5</sub> and surface desorption of HNO<sub>3</sub> in a large Teflon chamber, *Geophys. Res. Lett.*, *25*, 2169–2172, doi:10.1029/98GL51596.
- Wahner, A., T. F. Mentel, M. Sohn, and J. Stier (1998b), Heterogeneous reaction of N<sub>2</sub>O<sub>5</sub> on sodium nitrate aerosol, *J. Geophys. Res.*, *103*(D23), 31,103–31,112, doi:10.1029/1998JD100022.
- Wayne, R. P., et al. (1991), The nitrate radical: Physics, chemistry, and the atmosphere, *Atmos. Environ.*, *25A*, 1–203.
- 
- T. Anttila, Climate and Global Change, Research and Development, Finnish Meteorological Institute, FIN-00101 Helsinki, Finland.
- A. Kiendler-Scharr and T. F. Mentel, ICG-II: Troposphere, Forschungszentrum Jülich, D-52425 Jülich, Germany.
- N. Riemer, Department of Atmospheric Sciences, University of Illinois at Urbana-Champaign, 105 South Gregory Street, Urbana, IL 61801, USA. (nriemer@illinois.edu)
- B. Vogel and H. Vogel, Institut für Meteorologie und Klimaforschung, Forschungszentrum Karlsruhe, D-76344 Eggenstein-Leopoldshafen, Germany.